Biochimica et Biophysica Acta, 982 (1989) 228–236
Elsevier

BBAMEM 74475

Infrared and ^{31}P-NMR studies of the interaction of Mg^{2+} with phosphatidylserines: effect of hydrocarbon chain unsaturation *

H.L. Casal [1], H.H. Mantsch [1] and H. Hauser [2]

[1] *Division of Chemistry, National Research Council of Canada, Ottawa (Canada) and* [2] *Laboratorium für Biochemie, ETH-Zentrum, Zürich (Switzerland)*

(Received 20 December 1988)
(Revised manuscript received 11 April 1989)

Key words: Phosphatidylserine; Unsaturated fatty acid chain; Magnesium ion complex; Hydration; Fourier transform infrared spectroscopy; NMR, ^{31}P-

Infrared and ^{31}P-NMR spectra of aqueous dispersions of 1,2-dimyristoyl-*sn*-glycero-3-phospho-L-serine (DMPS), 1-palmitoyl-2-oleoyl-*sn*-glycero-3-phospho-L-serine (POPS), 1,2-dioleoyl-*sn*-glycero-3-phospho-L-serine (DOPS) and ox brain phosphatidylserine in the presence of excess Mg^{2+} have been recorded. A consistent picture emerges from the application of infrared and ^{31}P-NMR spectroscopy to Mg^{2+}–PS interactions. Mg^{2+} forms crystalline complexes with saturated phosphatidylserines, such as DMPS, and probably with POPS. In these crystalline PS-Mg^{2+} complexes the phosphate group loses its water of hydration but the serine carboxylate remains hydrated. Furthermore, there is formation of an additional hydrogen bond to one of the ester carbonyl groups of DMPS, and interchain interactions appear to be enhanced as reflected by a tighter packing of the fatty acyl chains. One main conclusion of this work is that Mg^{2+} binding to PS bilayers shows a gradation, the binding is in the order DMPS > POPS > ox brain PS > DOPS. The molecular area increases in the order DMPS < ox brain PS < POPS < DOPS and is apparently an important parameter determining the affinity of PS for Mg^{2+}. The general trend is that with increasing molecular area, and hence spacing of the ligands, the binding of Mg^{2+} decreases. While PS with two saturated fatty acyl chains forms tightly packed, crystalline Mg^{2+} complexes with an immobilized headgroup, the unsaturated PS molecules such as ox brain PS and DOPS interact only weakly with Mg^{2+}. Their interaction seems to be restricted to electrostatic shielding, since no major changes in molecular conformation, chain packing and headgroup hydration are found. The interaction of POPS with Mg^{2+} is intermediate between that of saturated PS and that of DOPS. POPS exhibits a higher affinity for Mg^{2+} than ox brain PS, although their molecular areas (and the surface charge density) are approximately the same. This apparent anomaly is proposed to be due to a discreteness of charge effect. It is proposed that a lipid surface with regularly spaced polar groups has a higher affinity for binding Mg^{2+}.

Introduction

PS is the major anionic phospholipid in many cell membranes. It is negatively charged under physiological conditions, and its interaction with mono- and divalent cations has been implicated in many membrane associated processes, such as lipid phase regulation and modulation, as well as related processes such as fusion events, enzyme regulation, signal transmission etc. Therefore, the interaction of physiologically important cations with PS model membranes has been the subject of extensive studies [1–22].

In this work we investigate the interaction of Mg^{2+} with well-defined synthetic phosphatidylserines differing in the degree of chain unsaturation and thus in the surface area occupied by each PS molecule at the lipid/water interface. Related to the area/molecule is the intermolecular separation of the charged groups ($-PO_4^-$, $-CO_2^-$, $-NH_3^+$) of PS that may be involved in the binding or chelating of the ion. By using the following series of synthetic phosphatidylserines, DMPS, POPS, DOPS, in which the number of unsaturated fatty acyl chains increases systematically, together with the naturally occurring ox brain PS, we explore the effect of

* Issued as NRCC publication No. 29986.

Abbreviations: PS, phosphatidylserine; DMPS, 1,2-dimyristoyl-*sn*-glycero-3-phospho-L-serine; POPS, 1-palmitoyl-2-oleoyl-*sn*-glycero-3-phospho-L-serine; DOPS, 1,2-dioleoyl-*sn*-glycero-3-phospho-L-serine; DSC, differential scanning calorimetry; Tes, 2-{[2-hydroxy-1,1-bis(hydroxymethyl)ethyl]amino}ethanesulfonic acid.

Correspondence: H.L. Casal, Division of Chemistry, National Research Council of Canada, Ottawa, Ontario, Canada K1A 0R6.

chain unsaturation on PS interactions with Mg^{2+}. The interaction of Mg^{2+} with different phosphatidylserines is compared to that with other cations, particularly Ca^{2+} and Li^{+}.

Experimental procedure

DMPS, POPS and DOPS were synthesized as described previously [23]. Bovine brain PS was purchased from Lipid Products (Surrey, U.K.) and used without further purification. All phospholipids used were pure as determined by TLC methods [24] and by chemical microanalysis. The acid form of PS was converted into the mono-ammonium salt as described before [24] or according to the method of Bligh and Dyer [25]. Alkali metal chlorides and $MgCl_2$ (Puriss grade) were obtained from Merck (Rahway, N.J.). All other chemicals were of analytical grade.

Samples for IR and ^{31}P-NMR measurements were prepared by evaporating a solution of the NH_4^+ salt of PS in $CHCl_3/CH_3OH$ (2:1, v/v) in a round-bottom flask and drying the lipid film in vacuo. Unless stated otherwise, the PS was dispersed in 5 mM Tris buffer prepared with double-distilled H_2O (pH 7.0) containing 0.05% NaN_3 for NMR measurements. For infrared measurements, the buffer (100 mM NaCl/2 mM Tes/2 mM His/0.1 mM EDTA (pH 7)) was prepared with H_2O or D_2O depending on the spectral region under investigation. Mixtures of the different phospholipids with $MgCl_2$ were prepared by adding a solution of $MgCl_2$ in the same buffer to a ready-made dispersion of the lipid. The addition was always carried out at temperatures above the corresponding gel-to-liquid crystal transition temperature of the phospholipid. Unless otherwise stated, the final PS concentration was 0.12–0.15 M for both IR and NMR measurements. For infrared measurements, $MgCl_2$ was added to obtain various PS/Mg^{2+} molar ratios. The $MgCl_2$ concentration in the ^{31}P-NMR sample was 1 M. High Mg^{2+} concentrations were used in order to shift the equilibrium towards the PS-Mg^{2+} complex. Some NMR samples were made by adding the $MgCl_2$ solution in buffer directly to the dry lipid film. The same results were obtained regardless of the method of sample preparation.

Infrared spectra at 2 cm^{-1} resolution were collected on a Digilab FTS-15 spectrometer equipped with a HgCdTe detector operated at 77 K. The samples were held in cells of 12 μm pathlength fitted with CaF_2 windows.

Proton-decoupled ^{31}P powder NMR spectra of PS and PS-Mg^{2+} complexes were recorded at room temperature on a Bruker CXP-300 Fourier transform spectrometer operating at a ^{31}P frequency of 121.46 MHz. Crystalline samples giving rise to axially asymmetric powder spectra were recorded with the cross-polarization, double-resonance technique [26]. For liquid crystalline phospholipid dispersions simple 90° pulses were used. Chemical shielding was referenced relative to external 85% orthophosphoric acid. The error in determining the width of axially asymmetric ^{31}P power spectra was 3–5 ppm, the error in the width of axially symmetric powder spectra was 1–3 ppm.

Results

In the presentation and discussion of the spectroscopic results we refer to PS dispersions containing Mg^{2+} as PS-Mg^{2+} regardless of whether a well-defined complex is formed between PS and the metal ion.

Infrared spectra

Infrared spectra of different PS molecules have been described in detail in previous publications, along with the specific effects associated with the binding of Li^+ and Ca^{2+} [20–22]. The thermal phase behaviour of DMPS dispersions in the presence of Mg^{2+} has been studied previously by DSC [18]. In samples containing increasing quantities of Mg^{2+} there appears a second order–disorder transition at higher temperature. At Mg^{2+}/DMPS molar ratios of less than 1.7 two transitions were observed in the DSC experiment, one at 40°C and one at 92°C [18]. The transition at 40°C corresponds to the gel-to-liquid crystal transition of uncomplexed DMPS, while the second at 92°C is assigned to the transition of the DMPS-Mg^{2+} complex.

The temperature-dependence of the infrared spectra of DMPS in the presence of equimolar amounts of Mg^{2+} is consistent with the previous DSC results. As shown in Fig. 1A, two discontinuities were observed in a plot of the wavenumber of the methylene symmetric stretching mode, $\nu_s(CH_2)$ versus temperature. As in the case of the DSC experiment, the first discontinuity, at 40°C, reflects the melting of the fatty acyl chains of the uncomplexed DMPS-NH_4^+, while the second discontinuity, in the range 84–90°C, reflects the corresponding transition of the DMPS-Mg^{2+} complex. The discontinuity at 40°C involves a shift of only 0.3 cm^{-1} in the $\nu_s(CH_2)$ wavenumber, while the one at higher temperatures induces a shift of 1.8 cm^{-1}. These spectral changes are similar to those found earlier in mixtures of DMPS with LiCl [21].

The data obtained from the infrared spectra of POPS mixed with $MgCl_2$ in equimolar amounts are quite different (Fig. 1B). In this case, there is a major change at 20°C, which corresponds to the gel-to-liquid crystal transition of POPS-NH_4^+ [22,27], and a second, much smaller change at 42°C. The first change at 20°C involves a shift in the $\nu_s(CH_2)$ wavenumber of 1.7 cm^{-1}, while the second change at 42°C comprises only a shift of 0.2 cm^{-1}. In analogy to DMPS (Fig. 1A), we conclude that POPS also forms a complex with Mg^{2+}

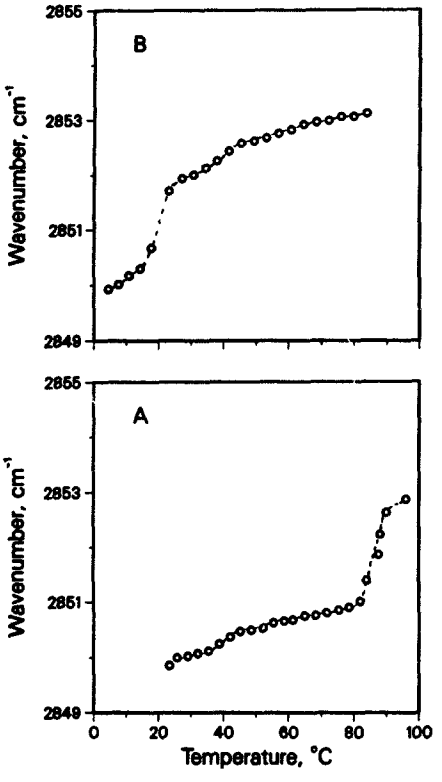

Fig. 1. Temperature-dependence of the wavenumber of the $\nu_s(CH_2)$ band in the infrared spectra of samples containing (A) 0.12 M DMPS-NH_4^+ and 0.12 M $MgCl_2$ and (B) 0.15 M POPS-NH_4^+ and 0.15 M $MgCl_2$. Samples were dispersed in buffer prepared with D_2O (pH 7.0) (see Experimental procedure).

with a transition at approx. 42°C. However, even though these plots cannot be used quantitatively, it would appear that in this 1:1 mixture the amount of uncomplexed POPS-NH_4^+ is much larger than that of POPS-Mg^{2+}.

The temperature-dependence of the $\nu_s(CH_2)$ mode in the spectra of DOPS in the presence of equimolar Mg^{2+} is identical to that of a sample of DOPS in the absence of Mg^{2+}. The same is true for ox brain PS. From this, and from the spectra discussed below, we conclude that DOPS and ox brain PS do not form a complex with Mg^{2+}.

Fig. 2 shows the 1800–1550 cm^{-1} region of the infrared spectra of DMPS-Mg^{2+}, POPS-Mg^{2+} and DOPS-Mg^{2+} at 52, 27 and 24°C, respectively. These temperatures were selected to be above the gel-to-liquid crystal transition temperatures of the lipids. This is particularly important in the case of POPS, as previous work [22] has shown that the affinity of this lipid for metal ions increases above its gel-to-liquid crystal transition. In each of the three spectra shown in Fig. 2 there is only one band in the range between 1700 and 1550 cm^{-1} due to the antisymmetric stretching of the serine carboxylate group $\nu_{as}(CO_2^-)$. The fact that there is only one band for the $\nu_{as}(CO_2^-)$ mode and that the wavenumber observed is in the range 1621–1625 cm^{-1}, is compatible with a well-hydrated carboxylate group in the three samples. Similar to Ca^{2+} binding, the interaction of Mg^{2+} with PS does not induce dehydration of the serine carboxylate group. This is contrasted by Li^+ binding to PS (DMPS, POPS, ox brain PS, see Refs. 21 and 22), in which case there appears a $\nu_{as}(CO_2^-)$ band at 1640 cm^{-1} [21], typical of dehydrated PS carboxylate groups. In the spectrum of ox brain PS in the presence of Mg^{2+} the $\nu_{as}(CO_2^-)$ mode also gives only one band at 1625 cm^{-1} (data not shown).

The bands due to the ester carbonyl groups in the region between 1800 and 1700 cm^{-1} differ considerably among the three spectra shown in Fig. 2. In the case of DMPS-Mg^{2+} there are three C = O stretching bands, at 1741, 1726 and 1711 cm^{-1}, while in the spectra of POPS-Mg^{2+} and DOPS-Mg^{2+} there are two main bands, at 1740 and 1730 cm^{-1}. Upon band narrowing (data not shown), a weak shoulder at 1711 cm^{-1} appears in the spectrum of POPS-Mg^{2+}. The spectrum of DOPS-

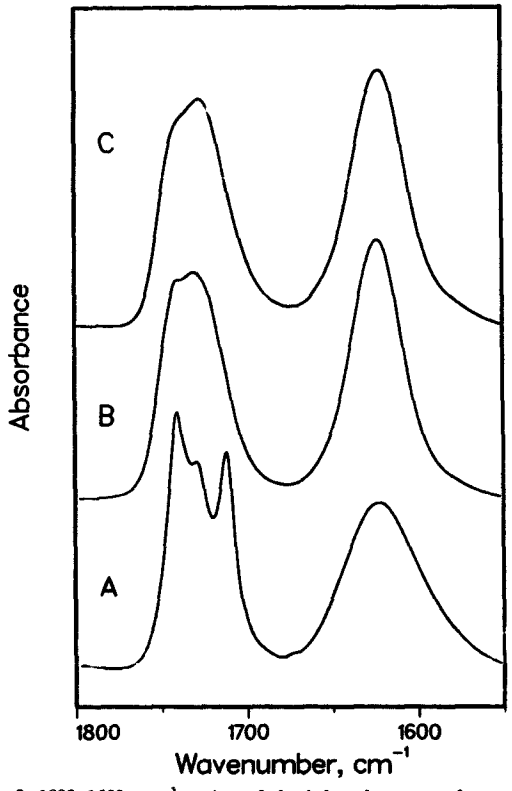

Fig. 2. 1800–1550 cm^{-1} region of the infrared spectra of aqueous dispersions of equimolar mixtures of (A) DMPS-NH_4^+ (0.12 M) and $MgCl_2$; (B) POPS-NH_4^+ (0.15 M) and $MgCl_2$; and (C) DOPS-NH_4^+ (0.15 M) and $MgCl_2$. Samples were dispersed in buffer (D_2O, pH 7.0).

Mg^{2+} is identical with the spectra of DOPS-Na^+ and DOPS-NH_4^+, supporting the conclusion that DOPS does not bind Mg^{2+}. Similarly, the spectrum of ox brain PS in the presence of Mg^{2+} is the same as that of the Na^+ salt and the same conclusion is reached as for DOPS.

In the infrared spectrum of DMPS-Mg^{2+} (Fig. 2) there is a C=O stretching band at 1711 cm^{-1}. This band is assigned to one of the ester C=O groups forming hydrogen bonds with two molecules of water, i.e., a disolvate [28]. In this respect, the spectrum of DMPS-Mg^{2+} resembles those of PS-Ca^{2+} complexes (cf. Fig. 8, Ref. 21 and Fig. 7, Ref. 22). In the spectra of DMPS-Ca^{2+}, POPS-Ca^{2+} and DOPS-Ca^{2+} the strongest C=O stretching band is that at the lowest frequency (1710, 1709 and 1702 cm^{-1}, respectively) and is assigned to a disolvate between one of the C=O groups and water [21,22]. In contrast, in the spectrum of DMPS-Mg^{2+}, the strongest C=O stretching band is that at 1741 cm^{-1} and not the band at 1711 cm^{-1}, assigned to a hydrogen-bonded C=O group. This shows that the extent of additional hydrogen-bonding induced by binding of Mg^{2+} is less than that induced by Ca^{2+} binding. Furthermore, the bandwidth of the C=O stretching band in the spectrum of DMPS-Mg^{2+} is 6.4 cm^{-1} as compared to 4 cm^{-1} measured in the spectrum of DMPS-Ca^{2+} [21]. Nevertheless, these bandwidths are quite narrow compared to other hydrogen-bonded ester C=O groups [28], demonstrating that in the DMPS-Mg^{2+} complex the ester moieties are immobilized. As in the case of PS-Ca^{2+} complexes, we propose that these hydrogen bonds are due to interstitial, trapped water molecules. The differences noted between the DMPS-Mg^{2+} and DMPS-Ca^{2+} complexes suggest that the binding of Mg^{2+} to PS is not as strong as that of Ca^{2+}. Similar conclusions were reached from ^{31}P-NMR studies (see below). The difference in affinity of Ca^{2+} and Mg^{2+} may be correlated with the difference in the fusogenic activity of these two metal ions [28,29]. It is important to stress that the spectrum of POPS-Mg^{2+} is intermediate between those of DMPS-Mg^{2+} and DOPS-Mg^{2+} or ox brain PS. There appears only a weak band at 1711 cm^{-1} in the spectrum of POPS (Fig. 2B), which may be associated with binding of Mg^{2+} to POPS.

The infrared spectra also indicate that binding of Mg^{2+} to the PS headgroup may induce dehydration of the phosphate group. Fig. 3 shows the 1300 to 1150 cm^{-1} region of the infrared spectra of DMPS-Mg^{2+}, POPS-Mg^{2+}, ox brain PS-Mg^{2+} and DOPS-Mg^{2+} at 52, 28, 26 and 23°C, respectively. In this region the antisymmetric double bond stretching, ν_{as}(O=P=O), of the phosphate group occurs, whose wavenumber may be used to determine the extent of hydration [30,31]. In the spectrum of DMPS-Mg^{2+} the ν_{as}(O=P=O) mode gives only one band at 1242 cm^{-1}. Two bands are observed at 1220 and 1240 cm^{-1} in the spectrum of POPS-Mg^{2+} and only one band, at 1220 cm^{-1}, in the spectra of ox

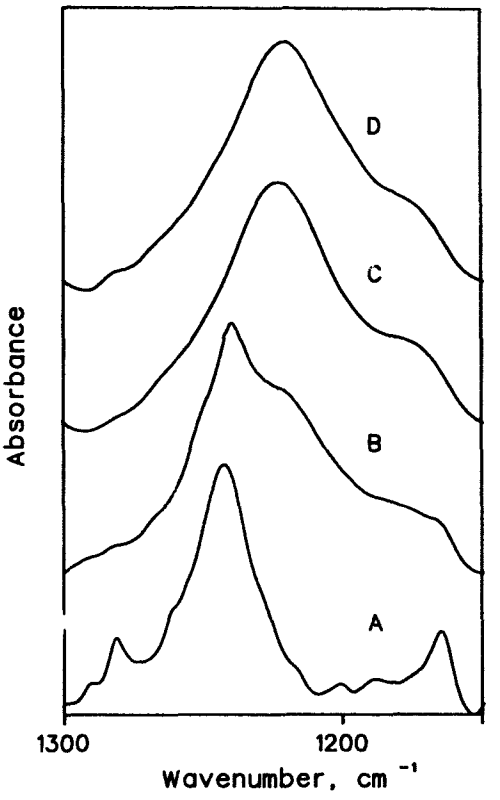

Fig. 3. 1300–1150 cm^{-1} region of the infrared spectra of aqueous dispersions of equimolar mixtures of (A) DMPS-NH_4^+ (0.12 M) and $MgCl_2$; (B) POPS-NH_4^+ (0.15 M) and $MgCl_2$; (C) Na^+ salt of ox brain PS (0.15 M) and $MgCl_2$ and (D) DOPS-NH_4^+ (0.15 M) and $MgCl_2$. Samples were dispersed in buffer (pH 7.0, H_2O).

brain PS-Mg^{2+} and DOPS-Mg^{2+}. These results demonstrate that in DMPS-Mg^{2+} the phosphate group is dehydrated, while in POPS-Mg^{2+} there are two POPS species, one with a dehydrated phosphate group (band at 1240 cm^{-1}) and one with a hydrated phosphate group (band at 1220 cm^{-1}). The two species may be assigned to the POPS-Mg^{2+} complex and to unchanged POPS, respectively. No evidence for dehydration of the phosphate group is found in the case of ox brain PS-Mg^{2+} and DOPS-Mg^{2+}. As noted above, the spectrum of POPS-Mg^{2+} is intermediate between those of DMPS-Mg^{2+} and DOPS-Mg^{2+}.

In the case of PS-Ca^{2+} complexes studied previously, a change in the conformation of the P–O bonds of the phosphate group was postulated [20] from *gauche-gauche* to antiplanar-antiplanar (or *gauche*-antiplanar). This was proposed from the appearance of a band at 665 cm^{-1} in the spectra of dried samples of PS-Ca^{2+} complexes. The spectrum of a dried sample of DMPS-Mg^{2+} does not show clear evidence of a change in conformation of the phosphate group. However, the region of the symmetric

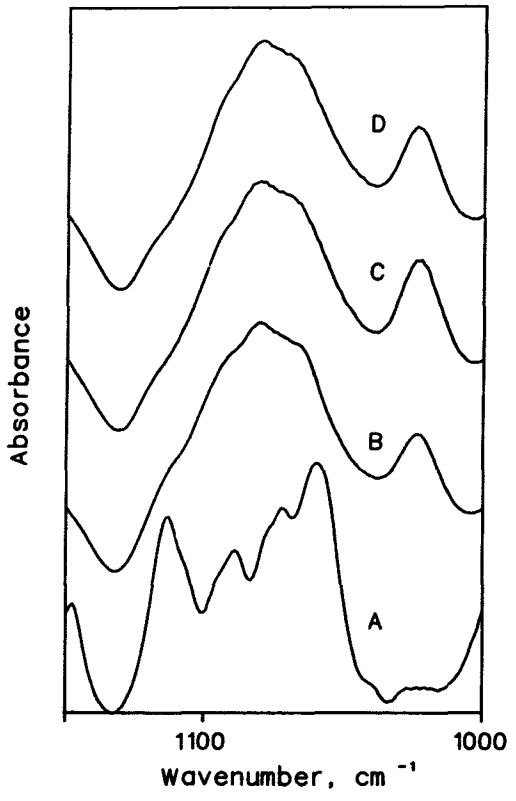

Fig. 4. 1150–1000 cm^{-1} region of the infrared spectra of aqueous dispersions of equimolar mixtures of (A) DMPS-NH_4^+ (0.12 M) and $MgCl_2$; (B) POPS-NH_4^+ (0.15 M) and $MgCl_2$; (C) Na^+ salt of ox brain PS (0.15 M) and $MgCl_2$ and (D) DOPS-NH_4^+ (0.15 M) and $MgCl_2$. Samples were dispersed in buffer (pH 7.0, D_2O). These spectra were recorded at the same temperature as those shown in Fig. 3.

double-bond stretching, ν_s(O=P=O), of the phosphate group in the spectrum of hydrated DMPS-Mg^{2+} (Fig. 4A) is similar to that of the PS-Ca^{2+} complex. This spectral region is shown in Fig. 4 for DMPS-Mg^{2+}, POPS-Mg^{2+} and DOPS-Mg^{2+}. In the spectrum of DMPS-Mg^{2+} there are four bands at 1114, 1090, 1075 and 1060 cm^{-1} in a pattern similar to that observed in the spectrum of DMPS-Ca^{2+} [20,21]. This is compatible with the formation of a Mg^{2+} complex (chelate) involving the phosphate group of DMPS. POPS-Mg^{2+} (Fig. 4B), ox brain PS-Mg^{2+} (Fig. 4C), and DOPS-Mg^{2+} (Fig. 4D) give similar infrared spectra with three main bands at 1090, 1080 and 1065 cm^{-1}. The shape of the bands in the spectra of POPS-Mg^{2+}, ox brain PS-Mg^{2+} and DOPS-Mg^{2+} is the same as that in the spectra of the respective NH_4^+ salts. This indicates that there is no strong interaction or chelate formation between Mg^{2+} and the phosphate group of the unsaturated PS molecules. This result, however, does not rule out electrostatic interactions between Mg^{2+} and their unsaturated PS bilayers. The fact that all PS bilayers are precipitated or salted out in the presence of excess Mg^{2+} demonstrates the existence of such an electrostatic interaction.

^{31}P-NMR spectra

Fig. 5 shows the proton-decoupled ^{31}P powder NMR spectra of the NH_4^+ salt of DMPS and the DMPS-Mg^{2+} complex. The NH_4^+ salt of DMPS dispersed in 5 mM Tris buffer (pH 7.0) gives rise to an axially symmetric ^{31}P powder pattern. At 25 °C the NH_4^+ salt of DMPS is in the gel state [24], characterized by a chemical shielding anisotropy of $|\Delta\sigma| = 79$ ppm (Fig. 5A). Above the transition temperature, T_c, which is 39 °C for the NH_4^+ salt of DMPS [17,24], the main feature of the axially symmetric ^{31}P powder NMR spectrum is retained, the chemical shielding anisotropy is, however, reduced to 57 ppm. Sometimes an isotropic signal is observed superimposed on the powder pattern (data not shown). The reduction in chemical shielding anisotropy $|\Delta\sigma|$ and the appearance of an isotropic signal at temperatures above T_c are due to a more effective motional averaging of the chemical shielding tensor in the liquid crystalline state.

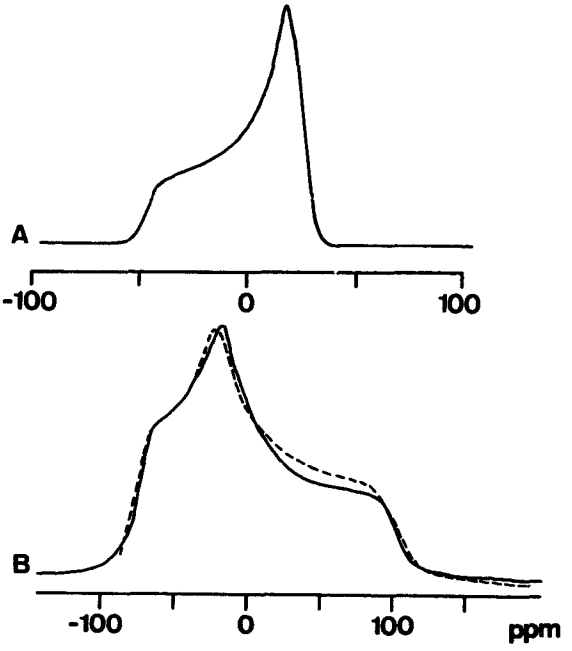

Fig. 5. Proton-decoupled ^{31}P powder NMR spectra of DMPS recorded at 121.46 MHz at 25 °C. (A) NH_4^+ salt of DMPS (0.144 M) dispersed in 5 mM Tris buffer (pH 7.0, 0.05% NaN_3). (B) Same dispersion as under (A) after addition of $MgCl_2$. With excess Mg^{2+} (final concn. approx. 1 M) an aqueous precipitate formed which was dried under N_2 for 24 h. The ^{31}P-NMR spectrum of this 'dry' precipitate is the solid curve. The dotted line is the ^{31}P-NMR spectrum of the aqueous precipitate of the Li^+ complex of DMPS formed by adding LiCl (approx. 1 M final concn.) to the aqueous dispersion described under (A). Chemical shielding is referenced relative to external 85% orthophosphoric acid.

The Na^+ salt of DMPS formed in the presence of 0.5 M NaCl gives an axially symmetric ^{31}P powder NMR spectrum at 25°C similar to that depicted in Fig. 5A with $|\Delta\sigma| = 80$ ppm (data not shown). Under these conditions, the Na^+ salt of DMPS precipitates and this precipitate suspended in the aqueous medium is referred to as aqueous precipitate (cf. Ref. 20). Addition of excess $MgCl_2$ (approx. 1 M) to the aqueous suspension of the NH_4^+ salt of DMPS in Tris buffer produces an aqueous precipitate of the DMPS-Mg^{2+} complex which gives rise to an axially asymmetric ^{31}P powder NMR spectrum. The signal-to-noise ratio of its spectrum was poor because of instrumental tuning problems. Therefore, the NMR spectrum shown in Fig. 5B (solid line) was recorded after removal of the mother liquor and drying the precipitate under N_2 for 24 h. The axially asymmetric ^{31}P powder pattern of this 'dry' DMPS-Mg^{2+} complex is identical within experimental error to that obtained from the aqueous precipitate of DMPS-Mg^{2+} (data not shown). It is also similar to that of the aqueous precipitate of DMPS in excess Li^+ (see dotted spectrum, Fig. 5B). The width of the axially asymmetric ^{31}P powder spectrum of DMPS-Mg^{2+} is $|\sigma_{11} - \sigma_{33}| = 185$ ppm, which agrees within experimental error with that of DMPS-Li^+ of 188 ppm [20]. The NH_4^+ salt of 1,2-dilauroyl-*sn*-glycero-3-phospho-L-serine behaves similarly; a dispersion in 5 mM Tris buffer (pH 7.0) at 30°C, which is about 17°C above the gel-to-liquid crystal transition temperatures [24], gives an axially symmetric ^{31}P powder NMR spectrum (data not shown). The lineshape and chemical shielding anisotropy $|\Delta\sigma| = 57$ ppm of this spectrum are very similar to the ^{31}P-NMR spectrum of DOPS at 25°C (Fig. 7C). In the presence of excess $MgCl_2$ (1.4 M) an aqueous precipitate forms which gives an axially asymmetric ^{31}P powder NMR spectrum similar to that of DMPS-Mg^{2+} shown in Fig. 5B.

The effect of excess Mg^{2+} on POPS bilayers is shown in Fig. 6. The Na^+-salt of POPS in the gel state (dispersed in 5 mM Tris buffer (pH 7.0) at 3°C) gives rise to an axially symmetric ^{31}P powder NMR spectrum with a chemical shielding anisotropy of $|\Delta\sigma| = 84$ ppm (Fig. 6A). Above the gel-to-liquid crystal transition temperature T_c, increased motional averaging reduces the chemical shielding anisotropy to $|\Delta\sigma| = 54$ ppm (Fig. 6B). In the presence of excess Mg^{2+} (approx. 1.4 M) an aqueous precipitate forms which gives an axially asymmetric ^{31}P powder pattern (Fig. 6C). The signal-to-noise ratio of the spectrum in Fig. 6C is not as good as that in Fig. 5B, hence the interpretation has been carried out cautiously. Although the width of this spectrum $|\sigma_{11} - \sigma_{33}| \approx 180$ ppm seems to be slightly reduced compared to that of DMPS-Mg^{2+}, the asymmetric shape of the spectrum is a clear indication of an immobilized phosphate group. We can conclude that the interaction of Mg^{2+} with POPS is similar to that of Mg^{2+} with

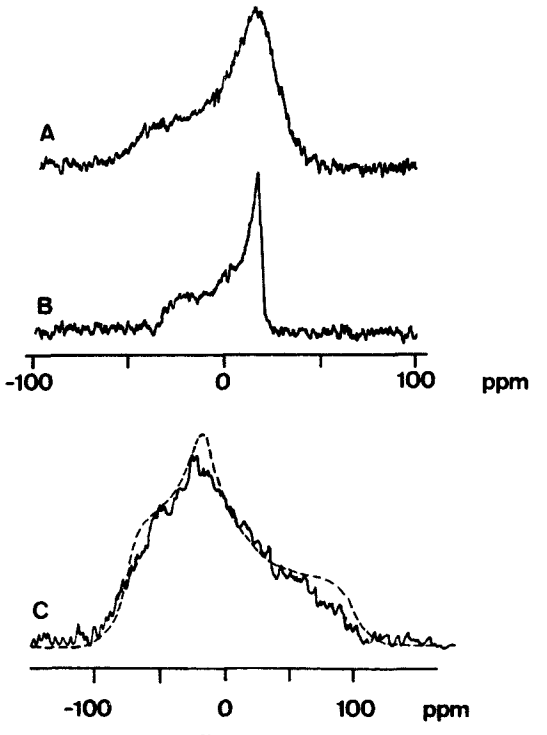

Fig. 6. Proton-decoupled ^{31}P powder NMR spectra recorded at 121.46 MHz. (A) Na^+ salt of POPS (0.062 M) dispersed in Tris buffer (5 mM pH 7.0, 0.05% NaN_3) recorded at 3°C. (B) The same dispersion as under (A) except that the ^{31}P-NMR spectrum was recorded at 25°C. (C) To the dispersion described under (A) $MgCl_2$ was added to a final concentration of 1.4 M. The dotted spectrum is that of DMPS-Mg^{2+} shown in Fig. 5B. Chemical shielding is referenced relative to external 85% orthophosphoric acid.

DMPS, leading to the immobilization of the lipid headgroup.

The effect of excess Mg^{2+} on DMPS and POPS is contrasted by the effect of Mg^{2+} on ox brain PS and DOPS. Fig. 7 shows proton-decoupled ^{31}P powder NMR spectra of the sodium salts of ox brain PS and DOPS in the presence and absence of Mg^{2+}. In contrast to DMPS, 1 M excess $MgCl_2$ has little effect on the axially symmetric ^{31}P powder spectra of the sodium salts of ox brain PS and DOPS. In the absence of Mg^{2+}, the chemical shielding anisotropies $|\Delta\sigma|$ derived from the axially symmetric ^{31}P powder spectra are $|\Delta\sigma| = 60$ ppm for ox brain PS (Fig. 7A) and $|\Delta\sigma| = 57$ ppm for DOPS (Fig. 7C). In the presence of 1 M $MgCl_2$, aqueous precipitates are formed with both ox brain PS and DOPS, which, in this respect, behave similarly to DMPS and POPS. The precipitation of PS dispersions in excess salt appears to be a general electrostatic phenomenon due to screening of the surface charge of PS. In contrast to DMPS-Mg^{2+} and POPS-Mg^{2+}, the aqueous precipitates of both ox brain PS and DOPS give axially sym-

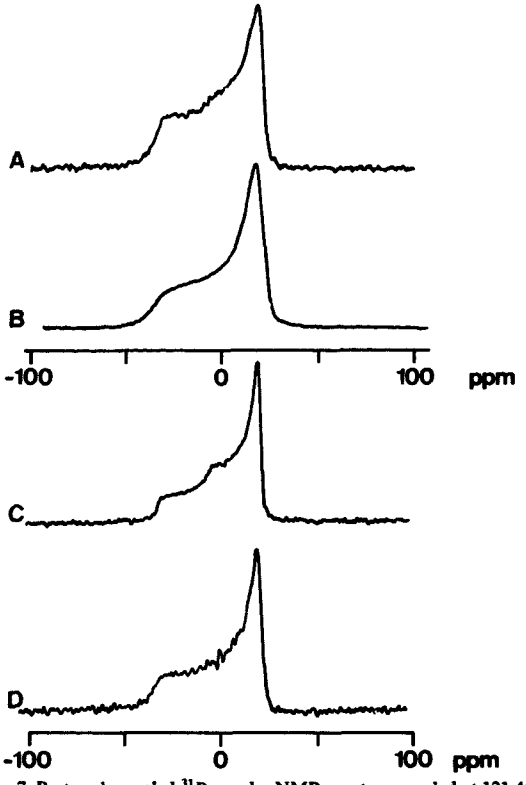

Fig. 7. Proton-decoupled ^{31}P powder NMR spectra recorded at 121.46 MHz at 25°C. (A) Na^+ salt of ox brain PS (0.40 M) dispersed in 5 mM Tris buffer (pH 7.0, 0.05% NaN_3). (B) To the dispersion described above $MgCl_2$ was added to a final concentration of 1 M and the spectrum of the aqueous precipitate was recorded. (C) Na^+ salt of DOPS (0.21 M) dispersed in the same Tris buffer. (D) To the dispersion described under (C) $MgCl_2$ was added to a final concentration of 1.4 M. Chemical shielding is referenced relative to external 85% orthophosphoric acid.

metric ^{31}P powder spectra with a chemical shielding anisotropy $|\Delta\sigma|$ only slightly increased by 2–3 ppm compared to the ^{31}P powder spectra in the absence of Mg^{2+} (cf. Figs. 7A–D). This result indicates that Mg^{2+} cannot interact strongly with either ox brain PS or DOPS. The ^{31}P-NMR spectra (Fig. 7) show that the presence of excess Mg^{2+} hardly affects the motion of the phosphate group of ox brain PS and DOPS.

Discussion

The data presented here describe the interaction of Mg^{2+} with PS differing in the degree of hydrocarbon chain unsaturation and some structural properties of the resulting PS-Mg^{2+} complexes. The main conclusion is that Mg^{2+} shows a gradation in its interaction with PS (DMPS > POPS > ox brain PS > DOPS). A consistent picture emerges from infrared and ^{31}P-NMR spectroscopy. Both methods emphasize the importance of the molecular area of PS and related to it, the surface charge density, in determining the affinity of PS for Mg^{2+}. The area per molecule increases from DMPS to DOPS; the values derived from surface pressure–area isotherms at 30 mN m^{-1} are 45.5 $Å^2$ for DMPS, 63.7 $Å^2$ for POPS, 62.0 $Å^2$ for ox brain PS, and 67.5 $Å^2$ for DOPS (PS monolayers were spread on 66 mM phosphate buffer (pH 7.4) at room temperature; from Ref. 27).

The molecular area apparently determines the separation of adjacent PS molecules and consequently the separation of ligands responsible for the chelation of the Mg^{2+} ion. The data presented show that, in general, as the PS molecular area increases, the affinity of PS for Mg^{2+} decreases. PS with two saturated hydrocarbon chains, such as dilauroylphosphatidylserine and DMPS, exhibit the highest affinity for Mg^{2+}. There is a dramatic decrease in affinity going from DMPS to POPS with one saturated and one unsaturated hydrocarbon chain. While saturated PS molecules form a tight complex (chelate) with Mg^{2+} [18], unsaturated PS like ox brain PS and DOPS do not form complexes even in the presence of a 5–10 fold excess of Mg^{2+}, and POPS exhibits an intermediate affinity between that of DMPS and DOPS. A similar gradation in affinity has been found for the interaction of Li^+ with different PS bilayers [20–22,33]. Our data are also consistent with the work of Feigenson [34]. This author measured binding constants for the interaction of Ca^{2+} with POPS, ox brain PS, and DOPS, more precisely for the formation of $Ca(PS)_2$ complexes in excess Ca^{2+}. Significant differences were observed in Ca^{2+} affinity among POPS, ox brain PS and DOPS. The Ca^{2+} concentrations in equilibrium with the $Ca(PS)_2$ precipitate were 0.14, 0.25–0.7 and 3 μM for POPS, ox brain PS and DOPS, respectively [34].

Some structural details of the PS-Mg^{2+} complexes can be derived from IR and ^{31}P-NMR spectroscopy. Both IR and ^{31}P-NMR spectra demonstrate that Mg^{2+} forms a tight, crystalline complex with saturated PS bilayers, e.g., with bilayers of dilauroyl PS and DMPS. This is consistent with previous X-ray work [18], which provided evidence for the crystallinity of PS-Mg^{2+} complexes. The infrared spectrum of DMPS-Mg^{2+} is similar to the infrared spectra of PS-Ca^{2+} complexes, hence the structural properties of DMPS-Mg^{2+} resemble those of the PS-Ca^{2+} complexes studied previously [18,20–22]. For example, in the spectrum of DMPS-Mg^{2+} there appears a band at 1711 cm^{-1} which is due to one of the ester carbonyl groups forming a strong hydrogen-bond with trapped (interstitial) water. The same was observed in the spectrum of DMPS-Ca^{2+} [21] regarding the appearance of the C=O stretching band; however, the band is sharper in the spectrum of DMPS-Ca^{2+}. This is interpreted to be a manifestation of 'weaker' binding in the case of Mg^{2+}.

Formation of the DMPS-Mg^{2+} complex is associated with increased interchain interactions, as revealed by the characteristics of the CH_2 deformation modes (not shown), and also with dehydration of the phosphate group. As shown in Fig. 3, the phosphate group of DMPS loses its water of hydration upon formation of the DMPS-Mg^{2+} complex. These observations are entirely consistent with previous results obtained by X-ray diffraction [18].

In PS-Ca^{2+} complexes we suggested that the torsion angles of the two P–O ester bonds have the antiplanar-antiplanar or *gauche*-antiplanar conformation instead of the usual *gauche-gauche* conformation [20]. Mg^{2+} binds directly to the phosphate group of DMPS as demonstrated by our ^{31}P-NMR and IR spectra; however, the conformation of the phosphate group remains *gauche-gauche* in the PS-Mg^{2+} complex.

The ^{31}P powder NMR spectrum of DMPS in the presence of Mg^{2+} is characteristic of an axially asymmetric ^{31}P chemical shielding tensor. The ^{31}P-NMR spectra of NH_4^+ or Na^+ salts of DMPS are axially symmetric both below and above the gel-to-liquid crystal transition. Thus, the ^{31}P chemical shielding tensor is axially averaged both in the gel and in the liquid-crystalline state. The axial averaging of the chemical shielding tensor must be due to rotation about one or several bonds of the lipid polar group. Rotational diffusion of the whole molecule is not possible in the gel phase because of the crystallization of the hydrocarbon chains [24]. Hence, molecular diffusion can be ruled out as a possible mechanism for axial averaging of the ^{31}P chemical shielding tensor. The binding of Mg^{2+} to the phosphate group of PS and the loss of water of hydration lead to an immobilized PS-Mg^{2+} chelate. In this structure the rotational freedom about various bonds of the lipid polar group is apparently lost. As a result, the chemical shielding tensor becomes axially asymmetric.

As mentioned above the properties of POPS-Mg^{2+} are intermediate between those of the DMPS-Mg^{2+} complex and those of ox brain PS and DOPS which seem to interact with Mg^{2+} merely electrostatically. The formation of a POPS-Mg^{2+} complex is manifested both in the IR and ^{31}P-NMR spectra. The infrared spectra (cf. Fig. 3) show that in a POPS/Mg^{2+} mixture of molar ratio 1 some phosphate groups remain hydrated. Thus, the infrared spectra demonstrate that free, hydrated POPS coexists with the POPS-Mg^{2+} which contains dehydrated phosphate groups. At the same time, the temperature-dependence of the $\nu_s(CH_2)$ mode also gives an indication of Mg^{2+} binding to POPS. The ^{31}P-NMR spectrum of POPS in the presence of a large excess of $MgCl_2$ (Mg^{2+}/POPS, 22:1 molar ratio, cf. Fig. 6C) does not show any evidence of free POPS; this is due to the very large excess of Mg^{2+} used. In such a situation, the equilibrium will be shifted towards the POPS-Mg^{2+} complex. The lineshape of the ^{31}P-NMR spectrum is characteristic of an immobilized lipid headgroup.

The main factor determining affinity of the lipid for Mg^{2+} is the separation between the different functional groups responsible for binding the ion. This separation is determined by the cross-sectional area of each lipid molecule. Thus, the difference in the affinity of POPS and ox brain PS for Mg^{2+} seems surprising and merits comment. The molecular area of POPS is 63.7 $Å^2$ and that of ox brain PS is 62.0 $Å^2$ determined at pH 7.4 and 30 $mN \cdot m^{-1}$ from surface pressure versus area curves [27]. The molecular area of ox brain PS is slightly less than that of POPS and therefore equal affinity (or a slightly higher one) towards Mg^{2+} would be expected if intermolecular separation (spacing) was the only variable determining affinity. However, the opposite is observed; the IR (cf. Fig. 3) and ^{31}P-NMR spectra (Fig. 6) show clearly that Mg^{2+} induces spectral changes in POPS and not in ox brain PS. We have no ready explanation for this observation. A possible way of rationalizing the difference in Mg^{2+} binding between POPS and ox brain PS would be the following. As mentioned above, the average molecular areas of the two PS molecules are practically identical and so are the average charge densities, however, the actual spacing between the ligand groups responsible for binding of the Mg^{2+} ion may be different in the two cases. POPS forms a bilayer with regularly spaced ligands because of the chemical homogeneity of its fatty acyl chains. In contrast, due to their heterogeneity in fatty acid content, ox brain PS bilayers lack this regular spacing. Therefore, in this case, the distance between ligand groups varies significantly; this phenomenon of the discreteness of the ligand and hence the charges could account for the lack of Mg^{2+} binding of ox brain PS. It has been argued in the past that metal ion binding to phospholipid monolayers and bilayers is adequately described by the Gouy-Chapman-Stern theory [35–37] and that the discreteness of charges has a negligible effect [38,39]. This notion is correct to a first approximation. However, the clear-cut differences in Mg^{2+} binding to POPS and ox brain PS bilayers are difficult to reconcile with this theory which assumes the charges to be evenly distributed over the bilayer surface. The difference in the Mg^{2+} binding of POPS and ox brain PS is a manifestation of the importance of discrete, localized charges.

In summary, the present work confirms observations made earlier [21,22] regarding the importance of the lipid molecular area in determining the affinity towards binding of metal ions. The molecular area determines the separation of adjacent PS molecules and related to it, the separation of ligands responsible for the chelation of the Mg^{2+} ion. The present data also point out that, in the case of Mg^{2+}, the regular spacing of the lipid headgroups on the lipid surface facilitates interaction

with the ion. In previous studies, a gradation of affinity of PS towards Li^+ was found, but no detectable differences between POPS and ox brain PS. The interaction of Mg^{2+} with PS is, if structurally similar, weaker than that of Ca^{2+}. Ca^{2+} forms tight crystalline complexes with all the PS molecules studied here, from DMPS to DOPS, while Mg^{2+} can do so only with DMPS. This conclusion is in accord with previous studies that detected weaker binding of Mg^{2+} compared to binding of Ca^{2+}. The differences, which are attributed to the fact that the magnesium ion is more hydrated than the calcium ion, correlate well with the different fusogenic activity of Ca^{2+} and Mg^{2+} [29].

Acknowledgements

We thank Mrs. A. Martin for her assistance in recording infrared spectra. This work was supported by the Swiss National Science Foundation (Grant No. 31-25719.88).

References

1 Abramson, M.B., Katzman, R. and Gregor, H.P. (1964) J. Biol. Chem. 239, 70-76.
2 Papahadjopoulos, D. and Miller, N. (1967) Biochim. Biophys. Acta 134, 624-638.
3 Hauser, H. and Phillips, M.C. (1973) J. Biol. Chem. 248, 8585-8591.
4 Atkinson, D., Hauser, H., Shipley, G.G. and Stubbs, J.M. (1974) Biochim. Biophys. Acta 339, 10-29.
5 Jacobson, K. and Papahadjopoulos, D. (1975) Biochemistry 14, 152-161.
6 Puskin, J.S. (1977) J. Membr. Biol. 35, 39-55.
7 Hauser, H., Finer, E.G. and Darke, A. (1977) Biochem. Biophys. Res. Commun. 76, 267-274.
8 Papahadjopoulos, D., Vail, W.J., Newton, C., Nir, S., Jacobson, K., Poste, G. and Lazo, R. (1977) Biochim. Biophys. Acta 465, 579-598.
9 Papahadjopoulos, D., Portis, A. and Pangborn, W. (1978) Ann. N.Y. Acad. Sci. 308, 50-63.
10 Newton, C., Pangborn, W., Nir, S. and Papahadjopoulos, D. (1978) Biochim. Biophys. Acta 506, 281-287.
11 Ohki, S. and Kurland, R. (1981) Biochim. Biophys. Acta 645, 170-176.
12 Eisenberg, M., Gresalfi, T., Riccio, T. and McLaughlin, S. (1979) Biochemistry 18, 5213-5223.
13 McLaughlin, S., Mulrine, N., Gresalfi, T., Vaio, G. and McLaughlin, A. (1981) J. Gen. Physiol. 77, 445-473.
14 Ohki, S., Düzgüneş, N. and Leonards, K. (1982) Biochemistry 21, 2127-2133.
15 Loosley-Millman, M.E., Rand, R.P. and Parsegian, V.A. (1982) Biophys. J. 40, 221-233.
16 Hauser, H. and Shipley, G.G. (1981) J. Biol. Chem. 256, 11377-11380.
17 Hauser, H. and Shipley, G.G. (1983) Biochemistry 22, 2171-2178.
18 Hauser, H. and Shipley, G.G. (1984) Biochemistry 23, 34-41.
19 Cevc, G., Seddon, J.M. and Marsh, D. (1985) Biochim. Biophys. Acta 814, 141-150.
20 Casal, H.L., Mantsch, H.H., Paltauf, F. and Hauser, H. (1987) Biochim. Biophys. Acta 919, 275-286.
21 Casal, H.L., Mantsch, H.H. and Hauser, H. (1987) Biochemistry 26, 4408-4416.
22 Casal, H.L., Martin, A., Mantsch, H.H., Paltauf, F. and Hauser, H. (1987) Biochemistry 26, 7395-7401.
23 Hermetter, A., Paltauf, F. and Hauser, H. (1982) Chem. Phys. Lipids 30, 35-45.
24 Hauser, H., Paltauf, F. and Shipley, G.G. (1982) Biochemistry 21, 1061-1067.
25 Bligh, E.G. and Dyer, W.J. (1959) Can. J. Biochem. Physiol. 37, 911-917.
26 Pines, A., Gibby, M.G. and Waugh, J.S. (1973) J. Chem. Phys. 59, 569-590.
27 Demel, R.A., Paltauf, F. and Hauser, H. (1987) Biochemistry 26, 8659-8665.
28 Blume, A., Hübner, W. and Messner, G. (1988) Biochemistry 27, 8239-8249.
29 Wilschut, J., Düzgüneş, N. and Papahadjopoulos, D. (1981) Biochemistry 20, 3126-3133.
30 Arrondo, J.L.R., Goni, F.M. and Macarulla, J.M. (1984) Biochim. Biophys. Acta 794, 165-168.
31 Mushayakarara, E., Albon, N. and Levin, I.W. (1982) Biochim. Biophys. Acta 686, 153-159.
32 Dluhy, R.A., Cameron, D.G., Mantsch, H.H. and Mendelsohn, R. (1983) Biochemistry 22, 6318-6325.
33 Mattai, J., Hauser, H., Demel, R.D. and Shipley, G.G. (1989) Biochemistry, 28, 2322-2330.
34 Feigenson, G.W. (1986) Biochemistry 25, 5819-5825.
35 McLaughlin, S. (1977) Curr. Top. Membr. Transp. 9, 71-74.
36 Altenbach, G. and Seelig, J. (1984) Biochemistry 23, 3913-3920.
37 MacDonald, P.M. and Seelig, J. (1987) Biochemistry 26, 1231-1240.
38 Winiski, A.P., McLaughlin, A.C., McDaniel, R.V., Eisenberg, M. and McLaughlin, S. (1986) Biochemistry 25, 8206-8214.
39 Hartsel, S.C. and Cafiso, D.S. (1986) Biochemistry 25, 8214-8219.